INT. J. NUM. METH. HEAT FLUID FLOW, VOL 2, 517–535 (1992)

A TRANSIENT FINITE ELEMENT ADAPTATION SCHEME FOR THERMAL PROBLEMS WITH STEEP GRADIENTS

R. RAMAKRISHNAN

Analytical Services and Materials, Inc., M.S. 156, NASA Langley Research Center, Hampton, Virginia 23665, USA

ALLAN R. WIETING

NASA Langley Research Center, Hampton, Virginia, USA

AND

EARL A. THORNTON

University of Virginia, Charlottesville, Virginia, USA

ABSTRACT

An adaptive mesh refinement procedure that uses nodeless variables and quadratic interpolation functions is presented for analysing transient thermal problems. A temperature based finite element scheme with Crank–Nicolson time marching is used to obtain the thermal solution. The strategies used for mesh adaptation, computing refinement indicators, and time marching are described. Examples in one and two dimensions are presented and comparisons are made with exact solutions. The effectiveness of this procedure for transient thermal analysis is reflected in good solution accuracy, reduction in number of elements used, and computational efficiency.

KEY WORDS Aerodynamic heating Mesh adaptation Finite element scheme

NOMENCLATURE

c	= specific heat
c_S	= time step factor
$[C]$	= element capacitance matrix
k	= thermal conductivity
$[K]$	= element conductance matrix
L	= element length, (2), area coordinate, (9)
n	= number of nodes
$[N]$	= element interpolation functions
q_i	= components of heat flux rate vector
Q	= internal heat generation rate
r_i	= refinement indicator
$\{R\}$	= load vector
t	= time
T	= temperature in K
T_f	= temperature = $1.8*T - 460$

0961–5539/92/060517–19$2.00

Received February 1992
Revised June 1992

x, y = global coordinates
x_f = global coordinate = $x/0.0254$
y_f = global coordinate = $y/0.0254$
$\Delta x, \Delta y$ = mesh spacings along x, y coordinates
Δt = time step
α = threshold for refinement
β = threshold for derefinement
ξ, η = local coordinates
Δ = element area
∇ = gradient operator
ρ = density
κ = thermal diffusivity = $k/\rho c$
θ = parameter for transient scheme
Ω = domain of interest

Subscripts

av = average value
i = element index, (12)
ini = initial value
j = index for nodes
m = maximum value
ref = time between refinements
x, y = coordinate directions

Superscripts

e = element value
n = time step index

INTRODUCTION

Accurate determination of structural temperature response due to thermal loads is of critical importance in high-speed aerospace vehicle design. Advanced vehicles such as the National Aerospace Plane are envisaged to travel at speeds exceeding Mach 15. At these speeds, aerodynamic heating on body surfaces can produce high temperature gradients and attendant thermal stresses that have a major impact on the performance of such vehicles. The need to accurately predict deformations and stresses points to the development of improved thermal and structural analysis procedures. These procedures should include the capability to describe steep temperature gradients that vary temporally and spatially.

Finite element methods have proven to be effective tools for thermal and structural analyses[1]. In predicting temperature response, basic thermal elements are normally formulated assuming a linear temperature distribution. Hence, a large number of elements are needed in regions of severe gradients to accurately capture the non-linear temperature distributions. This is especially true for highly transient problems where the location of thermal loads can vary in space and time.

One of the main concerns for hypersonic flight is high localized thermal fluxes caused by the impingement of shocks generated by the vehicle nose or inlet compression ramps on engine cowl leading edges. An accurate prediction of temperature levels, gradients and attendant thermal stresses requires small mesh spacings at early times when thermal gradients are high and larger spacings when these gradients decrease due to conduction.

The methodology proposed in this paper uses a refinement scheme with element sizes being adapted at specified intervals to track time-dependent gradients. Finite elements with quadratic element interpolation functions are used in this adaptation procedure to enable accurate modelling of severe gradients with a minimal number of mesh points. The intent of this paper is to demonstrate the effectiveness of this new approach for accurately predicting the transient temperature response and its gradients due to aerodynamic heating.

MESH ADAPTATION

Mesh adaptation schemes that are commonly used are mesh movement, mesh enrichment, and mesh regeneration. Mesh movement schemes move the nodes to regions of high gradients while holding the number of elements in a mesh constant. Mesh enrichment consists of adding elements in regions where solution gradients are high. Mesh regeneration constructs an entirely new mesh based on solutions obtained on a previous mesh.

The use of mesh movement to predict steep temperature gradients for one dimensional transient thermal problems was presented by Hogge and Gerrekens[2]. This adaptive procedure used the concept of one-dimensional heat penetration depth which limits its applicability in multi-dimensions. An adaptive scheme for transient one-dimensional heat transfer which included mesh movement with local mesh refinement was detailed by Adjerid and Flaherty[3]. The use of an adaptive remeshing procedure using quadrilateral and triangular elements for two dimensional steady heat conduction was recently presented by Thornton and Vemaganti[4], and applications of a remeshing scheme using triangular elements for coupled fluid-thermal-structural applications was presented by Dechaumphai[5]. Convergence to steady state is achieved in these approaches by obtaining solutions on a succession of meshes with the finite element mesh being recreated at each adaptation. The use of an adaptive mesh refinement scheme using quadrilateral elements for analysing a class of linear elliptic boundary-value problems was presented by Demkowicz *et al.*[6]. The methodology described in the present paper uses adaptive enrichment and coarsening concepts to model transient heat transfer in one and two dimensions.

Adaptive procedure

A classical mesh refinement scheme in the context of the finite element method is the addition of elements in regions of high gradients. Elements that lie in these regions are identified by refinement indicators and subdivided. The rationale for using refinement indicators is that, while it is possible to predict the location of strong gradients for some thermal problems, the analyst in general does not have *a priori* knowledge of the location of these regions. All elements in the mesh that have indicators above a preset threshold value are enriched while those elements that have values below a threshold derefinement value are coarsened. On refinement of a typical element, the 'sub-elements' that result could be all quadrilaterals, or a combination of quadrilaterals and triangles. The number and type of the resulting sub-elements depend on the refinement level of the surrounding elements. The elements that result in a typical refinement and coarsening procedure are shown in *Figure 1*. The initial mesh with elements B, C and D to be refined is seen in *Figure 1a*. The mesh after refinement of these elements is shown in *Figure 1b*. If, on this refined mesh, element group C which includes elements C1, C2, C3 and C4, needs to be coarsened, the mesh obtained after derefinement appears in *Figure 1c*.

The method adopted in this paper is to complete an analysis on a given mesh and then refine the mesh at certain user-specified time intervals in the transient analysis. The refinement at this time is based on indicators computed on the solution obtained on the original mesh. Details of the adaptive refinement scheme used herein are found in Reference 7.

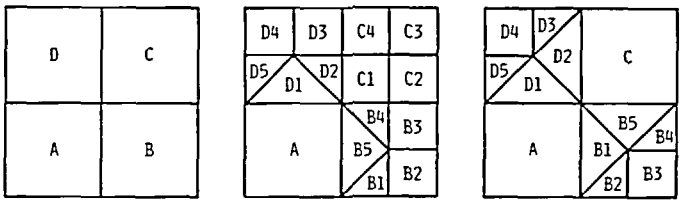

(a) (b) (c)

Figure 1 Adaptive refinement procedure. (a) Original mesh; (b) mesh after refinement of B, C and D; (c) mesh after coarsening of group C

The effectiveness of the transient adaptation procedure hinges on obtaining accurate temperatures at nodes created when elements are added and/or removed. Nodal temperatures of the newly created nodes are interpolated from the temperatures on the original mesh. Using elements with linear interpolation functions to model a domain yields inaccurate values for added nodes, especially those in regions of high gradients. These inaccuracies in turn have an adverse effect on the quality of the predicted transient response. Element distributions that yield better estimates for temperatures at newly created nodes are thus essential to model time dependent heat transfer.

Two ways to obtain a more realistic element temperature distribution are to use either higher order elements, which increases the number of nodes per element, or employ 'nodeless variable' elements which use hierarchical interpolation functions[8]. The advantage of the nodeless variable approach is that the geometric model used for finite element analyses is the same irrespective of the degree of polynomial used for element interpolation functions. The mesh that is employed for thermal analysis could also be used for structural analysis using either linear or nodeless variable elements.

NODELESS VARIABLE FINITE ELEMENTS

Dechaumphai and Thornton[8] developed nodeless variable quadrilateral finite elements for thermal and structural applications and demonstrated improved accuracy and efficiency in both applications. Elements may have one, two or more nodeless variables per element, depending on the order of the polynomial used to represent the element interpolation functions. The present effort employs one nodeless variable per element in one dimension, and three and four nodeless variables in two dimensions for triangular and quadrilateral elements respectively to obtain quadratic element temperature distributions.

One-dimensional nodeless variables

In one dimension, the temperature distribution for a linear element is given by:

$$T^e(x) = \sum_{i=1}^{2} N_i T_i \tag{1}$$

where T_i are the nodal temperatures and N_i are the interpolation functions given by:

$$N_1 = 1 - \frac{x}{L}$$

$$N_2 = \frac{x}{L} \tag{2}$$

where x is a local coordinate along the element length L. For a nodeless variable finite element with one nodeless variable, the temperature distribution is given by:

$$T^e(x) = \sum_{i=1}^{3} N_i T_i \tag{3}$$

where N_3 is the nodeless variable interpolation function given by:

$$N_3 = \frac{x}{L}\left(1 - \frac{x}{L}\right) \tag{4}$$

and T_3 is the nodeless variable temperature. The additional term in the element distribution in (3), associated with the nodeless variable T_3, allows for a non-linear description of the element temperature distribution. Temperature distributions for a one-dimensional element at various time intervals are shown in *Figure 2*. Distributions in a linear element are shown in *Figure 2a*, while the corresponding element temperature distributions using a finite element with one nodeless variable are shown in *Figure 2b*. The addition of the nodeless variable implies that the temperature variation within an element can change even if the nodal temperatures remain fixed. This situation could arise with internal heat generation or heat transfer on an element surface.

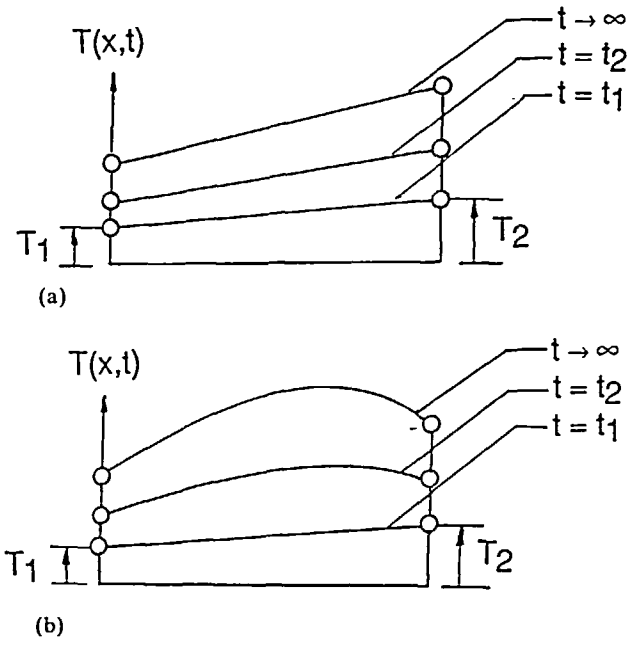

Figure 2 Element temperature distributions for one-dimensional (a) linear and (b) nodeless variable elements

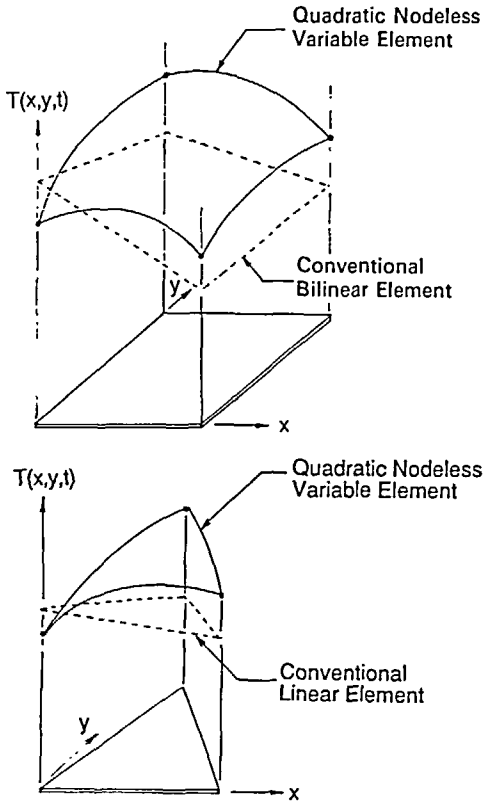

Figure 3 Schematics of temperature distribution for two-dimensional conventional and nodeless variable elements

Two-dimensional nodeless variables

The conventional four-node element with a general quadrilateral shape has bilinear element interpolation functions given by:

$$N_1 = \frac{(1-\xi)(1-\eta)}{4}$$

$$N_2 = \frac{(1+\xi)(1-\eta)}{4}$$

$$N_3 = \frac{(1+\xi)(1+\eta)}{4}$$

$$N_4 = \frac{(1-\xi)(1+\eta)}{4} \tag{5}$$

where ξ and η are local coordinates. The switch from global (x, y) coordinates to a local coordinate system is done to simplify evaluation of integrals over element areas or volumes. The local and global coordinate systems are related by:

$$x = \sum_{i=1}^{4} N_i(\xi, \eta) x_i$$

$$y = \sum_{i=1}^{4} N_i(\xi, \eta) y_i \tag{6}$$

In order to have a non-linear temperature distribution along the edges of an element as well as in its interior, nodeless variables are defined along element edges with edge interpolation functions given by:

$$N_5 = \frac{(1-\xi^2)(1-\eta)}{2}$$

$$N_6 = \frac{(1+\xi)(1-\eta^2)}{2}$$

$$N_7 = \frac{(1-\xi^2)(1+\eta)}{2}$$

$$N_8 = \frac{(1-\xi)(1-\eta^2)}{2} \tag{7}$$

where, for instance, N_5 varies quadratically between nodes 1 and 2 and is zero along the other three edges. The distribution of temperature for a typical nodeless variable quadrilateral element is given by:

$$T^e(x, y) = \sum_{i=1}^{4} N_i(\xi, \eta) T_i + \sum_{i=5}^{8} N_i(\xi, \eta) T_i \tag{8}$$

where N_1 to N_4 (5) are the same as the conventional bilinear interpolation functions, and N_5 to N_8 (7) are the nodeless variable quadratic interpolation functions.

For a linear triangular element, the interpolation functions are the same as the area coordinates

and the temperature variation along each element edge is linear. The area coordinates are given by[9]:

$$L_i = \frac{(a_i + b_i x + c_i y)}{2\Delta} \tag{9}$$

where Δ is the area of the triangle, and a_i, b_i and c_i are functions of nodal coordinates. To allow for a non-linear temperature variation along the edges of an element as well as its interior, nodeless variables are added along each edge. The quadratic interpolation functions for nodeless variable triangular elements are given by:

$$\begin{aligned} N_i &= L_i \qquad i = 1, 3 \\ N_4 &= 4L_1 L_2 \\ N_5 &= 4L_2 L_3 \\ N_6 &= 4L_3 L_1 \end{aligned} \tag{10}$$

The temperature distribution for a typical nodeless variable triangular element is:

$$T^e(x, y) = \sum_{i=1}^{3} N_i T_i + \sum_{i=4}^{6} N_i T_i \tag{11}$$

As with the quadrilateral elements, the shape functions at the physical nodes are exactly those of linear elements while N_4, N_5 and N_6 are the nodeless variable interpolation functions. Inter-element compatibility is preserved for adjacent elements by having a common nodeless variable on adjoining edges. Temperature distributions for typical quadrilateral and triangular elements with quadratic interpolation functions are contrasted with conventional quadrilateral and triangular elements in *Figure 3.*

Refinement indicators

The intent of the refinement procedure is to enhance solution quality by decreasing the size of key elements and improve efficiency by reducing the number of unknowns. The strategy adopted in this paper is to refine elements that lie in regions where the changes in temperature gradients are severe. For elements with interpolation functions given by (3), (8) and (11), the nodeless variable (or variables) in each element is a direct measure of deviation of the element temperature distribution from linear. For one-dimensional problems, the refinement indicator for a typical element is:

$$r_i = \frac{|T_3|}{T_{av}} \tag{12}$$

where T_3 is the nodeless variable temperature for that element and T_{av} is the average temperature in the element given by:

$$T_{av} = 0.5(T_1 + T_2) \tag{13}$$

The notion of using nodeless variables to define refinement indicators extends to two dimensions, with nodeless variables along element edges being a measure of the non-linear variation of temperature along those edges. In the case of a quadrilateral or triangular element, the maximum of the nodeless variables on element sides is taken as a refinement measure. For

a quadrilateral element the refinement indicator is computed as:

$$r_i = \frac{\max|T_j|}{T_{av}} \qquad j = 5, 8 \tag{14}$$

and T_{av} is the average element temperature based on the temperatures at the four physical nodes of the element.

The adaptive refinement procedure refines all elements that satisfy the criterion, $r_i > \alpha$, and derefines all elements that satisfy $r_i < \beta$, where α and β are preset refinement and derefinement threshold constants, respectively.

SOLUTION METHODOLOGY

The classical finite element approach for transient heat transfer is based upon using temperature as the dependent variable. A terse description of the problem statement, the finite element equations, and the time marching scheme follows.

Problem statement

Consider a solid bounded by surface $\delta\Omega$. The problem is governed by the energy equation,

$$\rho c(T)\frac{\partial T}{\partial t} + \frac{\partial q_i}{\partial x_i} - Q = 0 \tag{15}$$

where ρ is the density, c is the temperature dependent specific heat, q_i are components of the heat flux rate vector, and Q is the internal heat generation rate per unit volume. From Fourier's law,

$$q_i = -k_{ij}(T)\frac{\partial T}{\partial x_j} \tag{16}$$

where k_{ij} is the symmetric temperature dependent conductivity tensor. If Fourier's law is substituted into the energy equation, the parabolic transient heat conduction equation is obtained. This heat conduction equation is solved subject to appropriate initial and boundary conditions. An initial condition is specified throughout the domain and boundary conditions may take several forms such as specified temperature, specified heat flux rate, convective heat exchange, and radiative heat exchange.

Finite element equations

The solution domain is divided into elements and temperature and temperature gradients within an element are interpolated from nodal temperatures by:

$$T^e = [N]\{T\}$$
$$\nabla T^e = [\nabla N]\{T\} \tag{17}$$

where $[N]$ is a row matrix of the temperature interpolation functions. Using the method of weighted residuals[9] and integrating the heat flux gradient term by parts yields typical element equations of the form:

$$[C]\{\dot{T}\} + [K]\{T\} = \{R\} \tag{18}$$

where the capacitance matrix $[C]$ is given by:

$$[C] = \int_{\Omega} \rho c_p \{N\}[N]\, d\Omega \tag{19}$$

and the conductance matrix $[K]$ is given by:

$$[K] = \int_{\Omega} [\nabla N]^T [k][\nabla N]\, d\Omega \tag{20}$$

The element load vector $\{R\}$ is given by:

$$\{R\} = \int_{\Omega} Q\{N\}\, d\Omega \tag{21}$$

In one dimension, element capacitance and conductance matrices are 3×3 matrices for nodeless variable finite elements. In two dimensions, these matrices are 8×8 for a quadrilateral element and 6×6 for a triangular element. The finite element equations are assembled to form the global system of equations which is solved using a profile[10] solver.

Time marching scheme

The temperature formulation of non-linear heat transfer problems is described by (18). The transient solution is computed by a time marching method with an implicit, one parameter θ scheme[9] for time integration. If t_n is a typical time and t_θ is defined as $t_\theta = t_n + \theta\Delta t$ the element equations are written as,

$$[C]\{\dot{T}\}_\theta + [K]\{T\}_\theta = \{R\}_\theta \tag{22}$$

The Crank–Nicolson approximations are given by,

$$\{T\}_\theta = \frac{\{T\}^{n+1} - \{T\}^n}{\Delta t}$$

$$\{T\}_\theta = (1-\theta)\{T\}^n + \theta\{T\}^{n+1} \tag{23}$$

These approximations are introduced into (22) to yield the time marching procedure,

$$[[C] + \theta\Delta t[K]]_\theta\{T\}^{n+1} = [[C] - (1-\theta)\Delta t[K]]_\theta\{T\}^n + \Delta t\{R\}_\theta \tag{23}$$

which can be rewritten in 'delta' form as,

$$[[C] + \theta\Delta t[K]]\{\Delta T\}^{n+1} = -\Delta t[K]\{T\}^n + \Delta t\{R\} \tag{25}$$

The time marching procedure is unconditionally stable for $\theta \geqslant 0.5$ and conditionally stable for $\theta < 0.5$. Nodeless variable finite elements necessitate the use of the full capacitance matrix in (25), precluding explicit time stepping even for $\theta = 0$.

COMPUTATIONAL STRATEGIES

In transient heat transfer analyses, problems that have sudden changes in specified heat flux or temperature boundary conditions are common. Examples include shocks traversing the leading edge of a cowl of a hypersonic flight vehicle and laser-induced irradiations. To track transients accurately, two approaches are examined. The first approach uses a predictor–corrector concept while the second is a one-step approach which is less sophisticated but easier to implement.

For both approaches t_{ref} denotes the time when mesh adaptations are to be done and Δref the time between refinements. The thermal analysis is started at time t_{ini} and the maximum allowable time step is Δt_m. The value of Δt_m is reset inside the time marching procedure such that Δref is a multiple of the maximum allowable time step.

Approach 1

(1) At time t_{ini} for the initial mesh compute Δt_m
(2) Set index for refinement counter to zero
(3) Advance the solution to time t_{ref}
(4) Compute refinement indicators for the mesh based on temperature distribution at t_{ref}:
  (a) check maximum value of refinement indicator. If maximum value < preset limit, go to (8).
  (b) increment index: If index > preset maximum value, go to (8).
(5) Refine and/or coarsen the mesh based on the refinement indicators using the nodal values at time t_{ini}
(6) Calculate Δt_m and march the solution in time from t_{ini} to t_{ref}
(7) Go to step (4)
(8) Update:

$$t_{ini} = t_{ref}$$

$$t_{ref} = t_{ref} + \Delta\text{ref}$$

(9) Go to step (2)

The above approach yields good time accuracy since the solutions at any time are not stepped forward in time until preset refinement criteria are met. The drawbacks of the approach are that if the initial mesh used is crude repeated analysis will be needed at early time levels, and the preset limit of the refinement indicator sometimes has to be changed from problem to problem. An alternate approach that is less intensive and computationally more economical is detailed below.

Approach 2

(1) At time t_{ini} compute Δt_m
(2) Advance the solution to time t_{ref}
(3 Compute refinement indicators on the mesh based on temperature distribution at t_{ref}: check maximum value of refinement indicator. If maximum value < preset limit, go to (5).
(4) Refine and/or coarsen the mesh based on the refinement indicators using the nodal values at time t_{ref}
(5) Update:

$$t_{ini} = t_{ref}$$

$$t_{ref} = t_{ref} + \Delta\text{ref}$$

(6) Go to step (1)

A disadvantage of this approach is that inaccuracies may accumulate when thermal fluxes or temperature boundary conditions acting on a domain are highly transient in behaviour.

Time step estimation

The allowable time step Δt_m is restricted by the stability constraints and spatial accuracy requirements of the scheme. For one-dimensional heat conduction, with constant thermophysical

properties, the allowable time step is estimated by:

$$\Delta t_m = c_s(\Delta x)^2/2\kappa \tag{26}$$

where c_s is a time step factor that influences solution accuracy, κ the thermal diffusivity ($= k/\rho c$), and Δx the element length. Appropriate values for c_s depend on the time marching scheme used as well as the order of polynomials used for element interpolation functions. Examples of c_s values are given in the applications section. For two-dimensional heat conduction problems the maximum allowable time steps are calculated as:

$$\Delta t_m = c_s/[2\kappa_x/(\Delta x)^2 + 2\kappa_y/(\Delta y)^2] \tag{27}$$

where κ_x and κ_y are the diffusivities in the x and y directions.

Bandwidth minimization

An implicit set of global equations is formed by the assembly of element equations such as that given by (25). The global equations are solved at each time step by Gauss elimination. To decrease storage requirements global arrays for conductance and load are stored in profile form in columns above the principal diagonal. The full conductance matrix is not stored since the conductivity tensor is symmetric resulting in a symmetric global conductance matrix. The maximum column height of each node (or equation) is dependent on the element connectivity matrix, and, the storage requirements for the upper half of the global matrix is a function of the column heights of all equations.

The adaptive refinement scheme operates by enriching and coarsening a mesh. At each adaptation, nodes are added or removed, changing the element connectivity matrix. To reduce the storage requirement and increase computational efficiency, a bandwidth reduction scheme is used on the mesh obtained after each adaptation. A node numbering scheme assigns new nodal identities to existing nodes such that the difference in node numbers between related nodes for each element is decreased. This reduces the bandwidth of the global matrix and thus its storage requirements.

The bandwidth reduction scheme used is the one proposed by Collins[11], modified for elements with quadratic element interpolation functions. The scheme generates for each node in the mesh, a list of 'neighbour' nodes—a neighbour node being defined as a node that shares an element with this particular node. For an unstructured mesh the number of neighbouring nodes will vary depending on how many quadrilateral and triangular elements share this node. A node renumbering scheme is initiated with each node, in turn, being the starting point for this restructuring. The bandwidth for each renumbering scheme is compared during this renumbering procedure with the current minimum bandwidth and a scheme is abandoned whenever the bandwidth exceeds the minimum bandwidth calculated thus far. The number of renumbering schemes started is equal to the number of physical nodes in the domain. Nodes associated with the nodeless variables in elements are not considered as candidates for starting the renumbering scheme.

In the two-dimensional heat transfer examples presented in this paper, typical reductions in bandwidth ranges from factors of 10 to 20. This reduction in bandwidth reduces the storage requirements of the global arrays by factors up to 10.

APPLICATIONS

The effectiveness of the adaptive unstructured mesh refinement procedure for predicting transient temperature distributions is demonstrated for heat transfer problems in one and two dimensions.

In the examples presented transient heat conduction is modelled with fixed temperatures and specified heat flux boundary conditions. Internal heat generation is included and thermophysical properties are assumed constant for computational convenience. Nodal temperatures obtained from the finite element approach are compared with available exact solutions to arrive at nodal errors. These errors are used to measure the spatial and temporal accuracy of the adaptive scheme. The number of nodes used to model the domain, maximum allowable time step used, and temperature distributions obtained are monitored as the transients develop.

For the applications presented below the finite element mesh used at the initial time is uniform with small spatial dimensions. Small element sizes are needed to model high gradients that may be present very early in the thermal transient. Although the initial mesh is very fine over the entire domain, the adaptation scheme rapidly reduces the problem size by coarsening elements that are not located at regions of high gradients. The decision as to when and how much to adapt a mesh during the transient is based on the physics of the problem. If the initial mesh is fine and high gradients that exist during early transients are to be captured accurately, adaptations are not done very frequently during this period.

One-dimensional heat conduction

The problem statement for heat conduction in an aluminium strip is shown in *Figure 4*. The strip is initially at 295K and the right end of the strip is held at this temperature. The left end has a heat flux $q = 88.9\ \text{kW/m}^2$ applied at time zero, and the heat flux is held constant. Gradients develop in the strip gradually and the temperature distribution attains steady state given by a linear temperature profile. The physical properties of the strip are taken as:

$$\rho = 2712\ \text{kg/m}^3$$

$$c = 0.895\ \text{kJ/(kg K)}$$

$$k = 164.4\ \text{W/(m K)}$$

The mesh used to start the analysis has a uniform spacing of 2.38×10^{-3} m with the domain being modelled by 128 elements. Initially adaptations are done every 0.1 sec, and at the end of 1 sec, adaptations are done every 10 sec. The refinement and derefinement threshold values were set to 0.8 and 0.1 respectively. These threshold values were obtained as a result of numerical experimentation aimed at striking a balance between solution accuracy and minimizing number of elements used. The time marching strategy used for this example is 'Approach 1' described

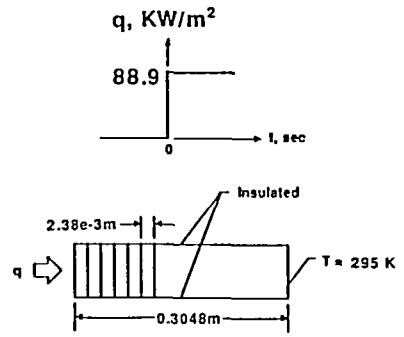

Figure 4. Problem statement for transient heat conduction in a strip

in the previous section. An iterative scheme[12] with $\theta = 0$ in (25), was used to march the solution out in time with the time step factor c_s set to 0.05. The low value of c_s is due to the quadratic interpolation functions used as well as the iterative scheme employed.

The temperature distributions at various instances in time are shown in *Figure 5* and the number of nodes, n, used at these times are also indicated. Exact nodal temperatures were obtained using a series expansion[13] and nodal errors are computed as the difference between exact and finite element temperatures at each node divided by the exact temperature at that node. Nodal errors in *Figure 6* indicate the maximum errors to be less than 0.5% throughout the analysis. The number of nodes in the finite element model during the transient response is plotted in *Figure 7* illustrating the rapid drop in the number of nodes very early in time. The number of nodes at time zero is seen to be 67. This is due to the fact that the maximum value of index for refinement counter in Approach 1 was set to unity. This causes the mesh to be adapted once, before the analysis is stepped forward in time. At 1 sec, the number of nodes needed to model the problem has already dropped down to less than ten. The maximum allowable time steps plotted as a function of time in *Figure 8* shows the increase in the time steps used as the gradients decrease due to conduction effects. The combination of decreased number of elements, and increased mesh spacings accelerates the solution to steady state while ensuring temporal accuracy. At 2000 sec, the temperature distribution is linear and the temperature at the left end is 459 K, which is within 0.05% of the exact calculations.

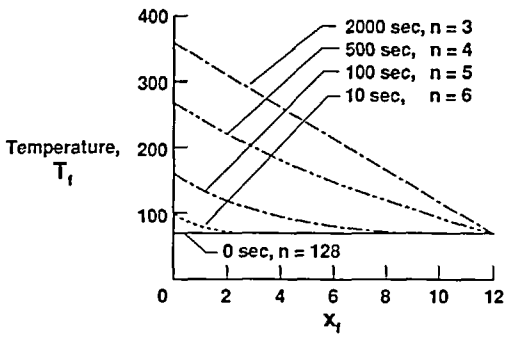

Figure 5 Temperature distributions at various time intervals

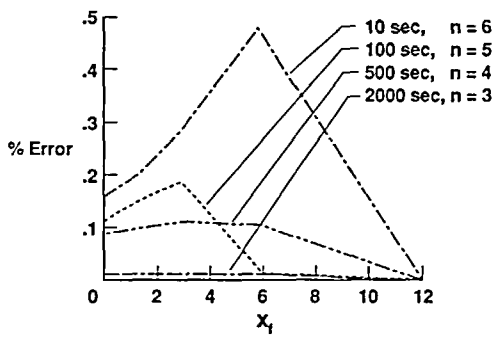

Figure 6 Nodal errors at various time intervals

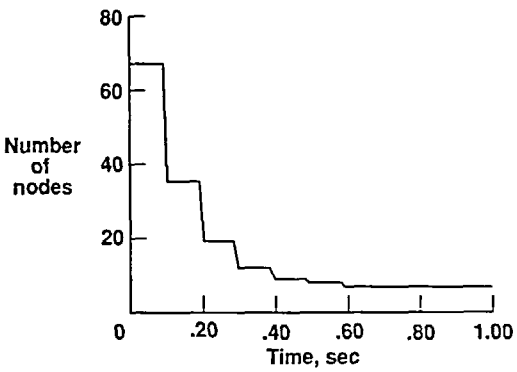

Figure 7 Nodes used for modelling domain as a function of elapsed time

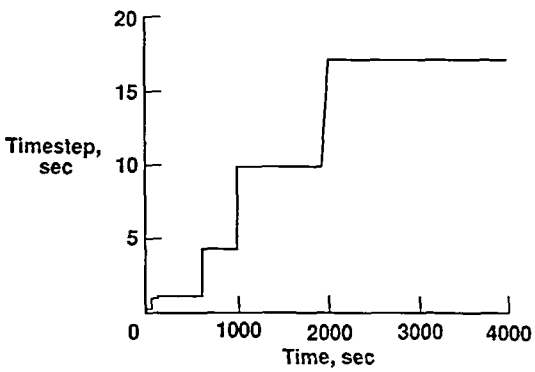

Figure 8 Time step used as a function of elapsed time

Two-dimensional heat conduction

Two examples illustrating heat transfer in two dimensional domains are presented. The first is a rectangular plate having a uniform temperature distribution initially. High gradients develop at the boundaries during the transient due to internal heat generation over the entire domain. Exact temperature distributions and temporal histories can be obtained for this problem[14], making it attractive for validating the adaptive finite element procedure. The second problem simulates a cylinder wall instantaneously heated over a small region and an idealized conduction model is used to obtain the transient temperature response. Both problems are marched out in time using 'Approach 2' described in the previous section.

Heat transfer in rectangular plate. The problem statement for heat conduction in a rectangular plate is shown in *Figure 9*. The boundaries of the plate are held at 255K and the internal heat

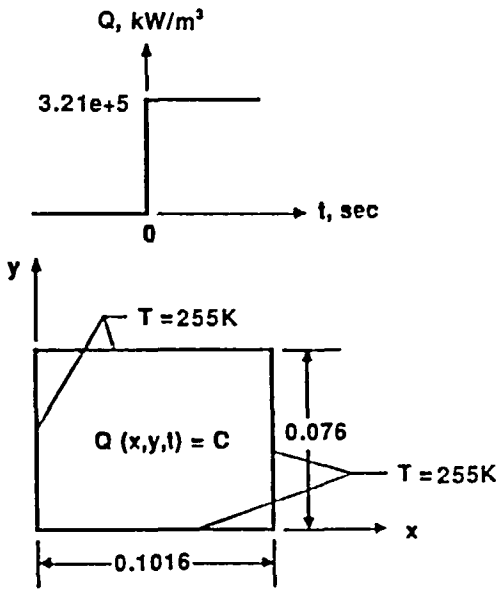

Figure 9 Problem statement for heat conduction in a rectangular plate

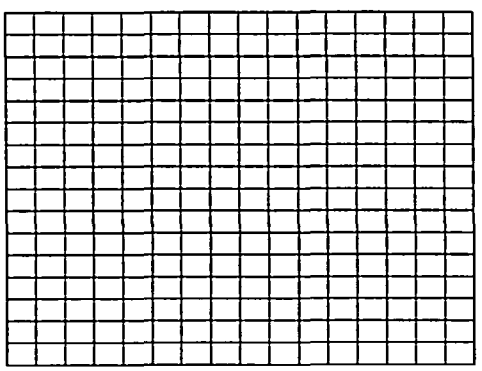

Figure 10 Initial mesh for heat transfer in rectangular plate

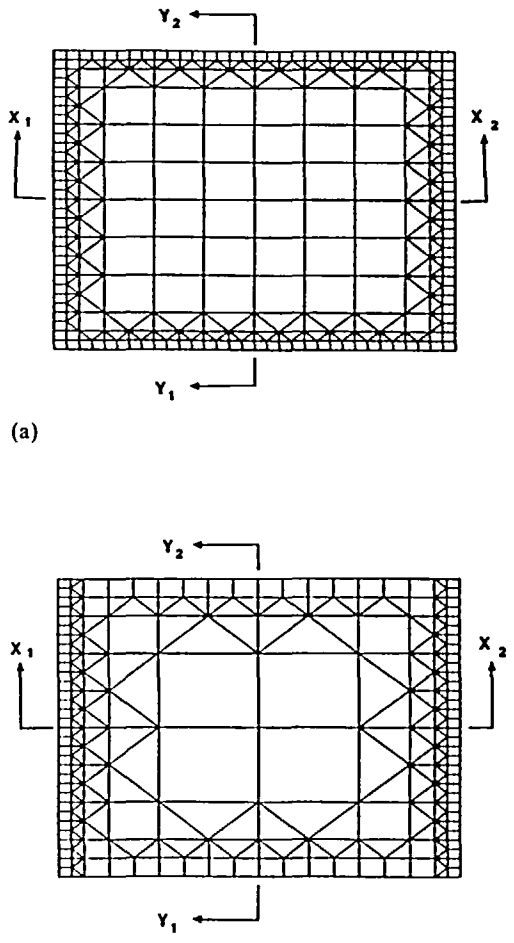

Figure 11 Finite element mesh for plate after (a) 0.3 sec and (b) 0.5 sec

generation rate for the domain is uniform and invariant at $3.21 \times 10^5\,\mathrm{kW/m^3}$. The plate is assumed to be at an uniform temperature of 255K at time zero and thermal properties of the plate are as follows:

$$\rho = 7800\,\mathrm{kg/m^3}$$

$$c = 0.7396\,\mathrm{kJ/(kg\,K)}$$

$$k = 248\,\mathrm{W/(m\,K)}$$

Sharp gradients exist near the boundaries at early time, and these gradients continue to be present as the temperature in the interior increases due to heat generation. Using symmetry conditions only one-fourth of the plate needs to be modelled but for this example the entire plate is considered.

The finite element mesh used to start the thermal analysis is shown in *Figure 10*. The mesh is adapted every 0.1 sec and the meshes at 0.3 and 0.5 sec are shown in *Figure 11*. Elements that lie along the boundaries are refined while elements at the centre of the domain are coarsened. The effectiveness of the adaptation procedure in modelling steep gradients at the boundaries is evaluated by examining the temperature distribution along section X_1–X_2 which passes through the centre of the plate. The temperature distribution and nodal errors at 0.5 sec along this line

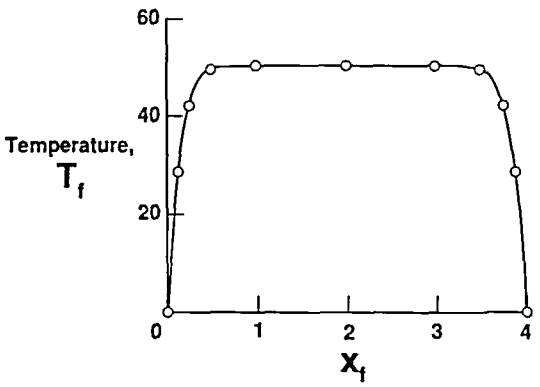

Figure 12 Temperature distribution along section X_1–X_2 at 0.5 sec

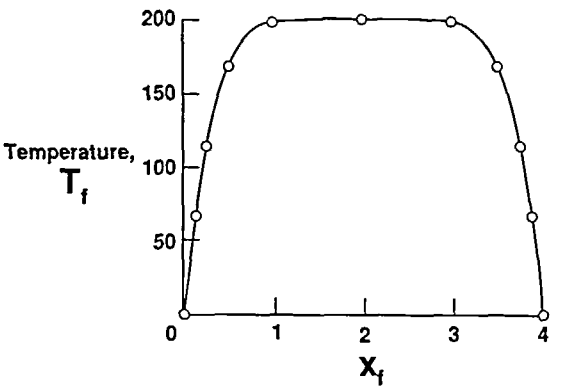

Figure 14 Temperature distribution along section X_1–X_2 at 2 sec

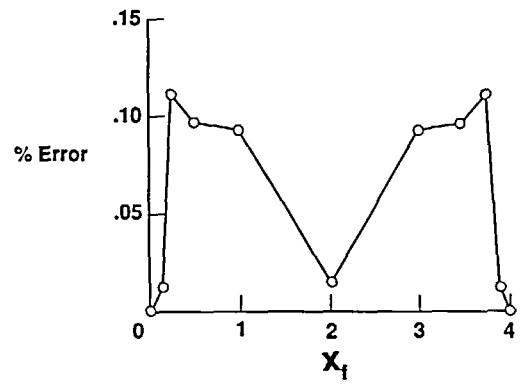

Figure 13 Nodal errors along section X_1–X_2 at 0.5 sec

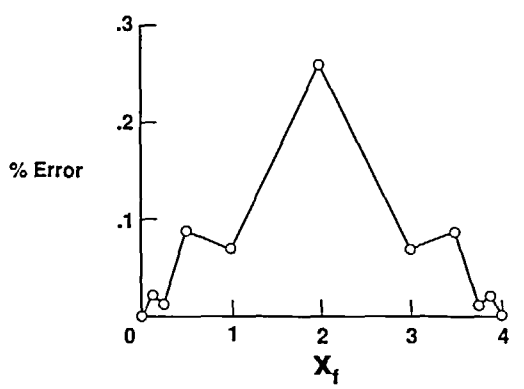

Figure 15 Nodal errors along section X_1–X_2 at 2 sec

are shown in *Figures 12* and *13*. The maximum error in the distribution is less than 0.15%. The finite element mesh at 2 sec is the same as that at 0.5 sec and the temperature profile and nodal errors at this time along section X_1–X_2 are shown in *Figures 14* and *15*. Again the maximum nodal error is less than 0.3% underlining the accuracy of the adaptation procedure. The time accuracy of the procedure was studied by marching the analysis in time up to 10 sec. Throughout the transients it was observed that the maximum error was less than 0.5%.

Aerothermal heating of leading edge. The effect of shock impingement and augmented heat loads on the surface of a high speed flight vehicle, shown in *Figure 16* is a problem of current interest. A rectangular domain, employing one-half symmetry about the x-axis, is a crude representation of a National Aerospace Plane leading edge subjected to intense local heating[15]. An idealization of the leading edge with temperature imposed over a small portion of the left boundary is analysed. The heated strip is held at 1000K. The initial and boundary conditions for the problem, as well as the initial mesh used for the analysis, are indicated in *Figure 17*. The leading edge is constructed from a nickel-based superalloy and physical properties of the

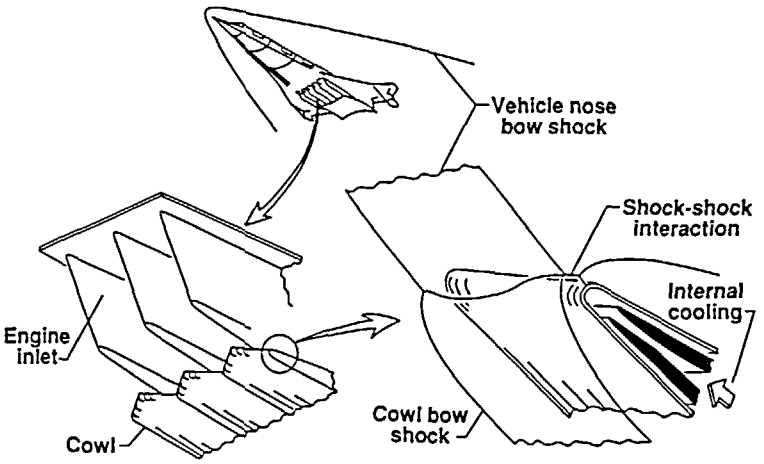

Figure 16 Schematic diagram of flow interaction on aerospace plane leading edge

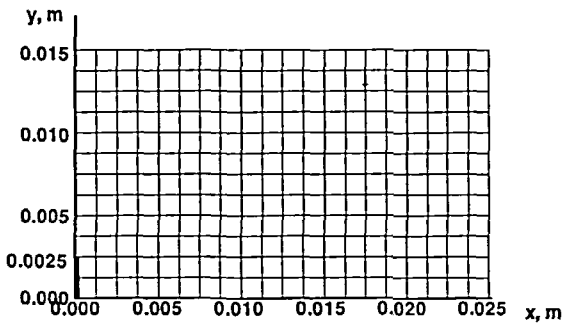

$T(0, y, t) = 1000\,\text{K}$ $\quad 0.0 < y < 0.0025$
$q_x(0, y, t) = 0$ $\quad 0.0025 < y < 0.0154$
$q_x(0.0254, y, t) = 0$ $\quad 0.0 < y < 0.0154$
$q_y(x, 0, t) = 0$ $\quad 0.0 < x < 0.0254$
$q_y(x, 0.0154, t) = 0$ $\quad 0.0 < x < 0.0254$
$T(x, y, 0) = 295\,\text{K}$

Figure 17 Problem statement and initial mesh for heat transfer on leading edge

superalloy were taken as:

$$\rho = 7800\,\text{kg/m}^3$$

$$c = 0.7396\,\text{kJ/(kg K)}$$

$$k = 248\,\text{W/(m K)}$$

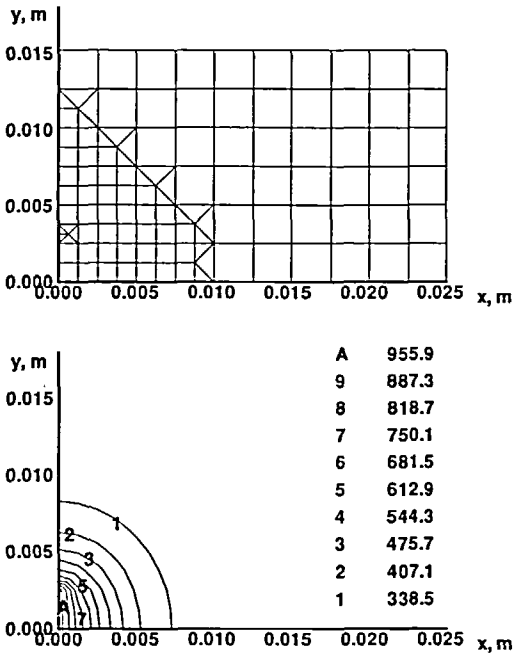

Figure 18 Finite element mesh and temperature distribution after 2.2 sec

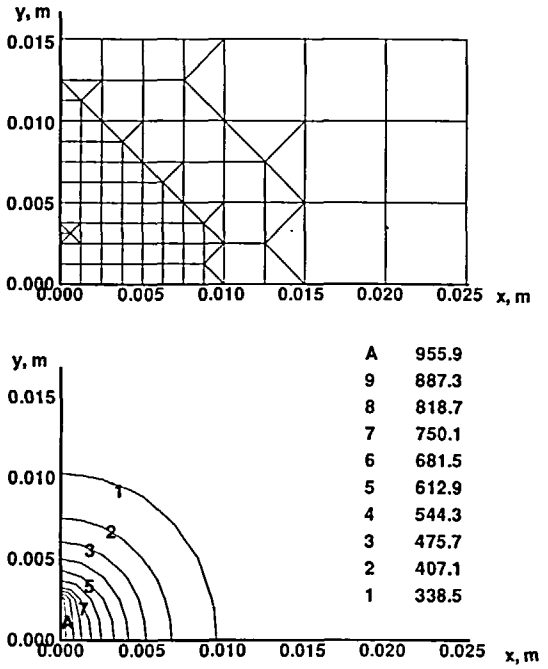

Figure 19 Finite element mesh and temperature distribution after 4.2 sec

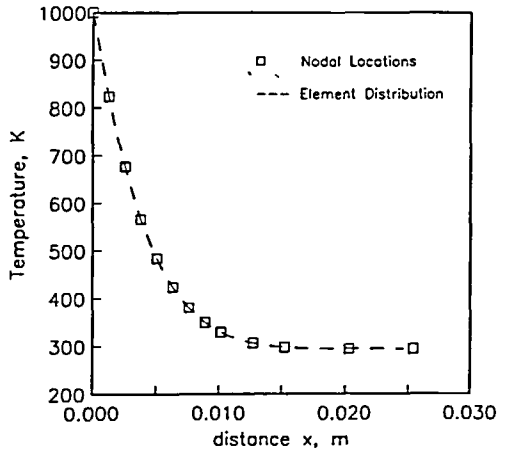

Figure 20 Temperature distribution along x-axis at 4.2 sec

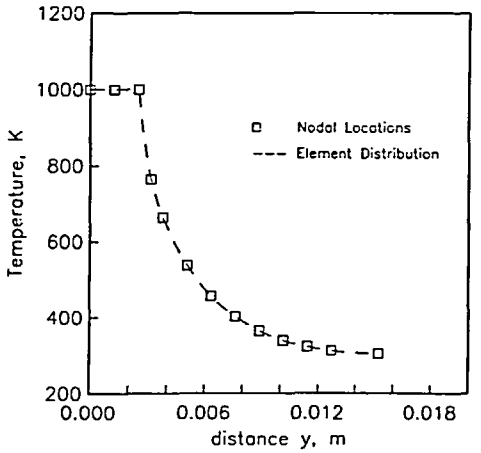

Figure 21 Temperature distribution along y-axis at 4.2 sec

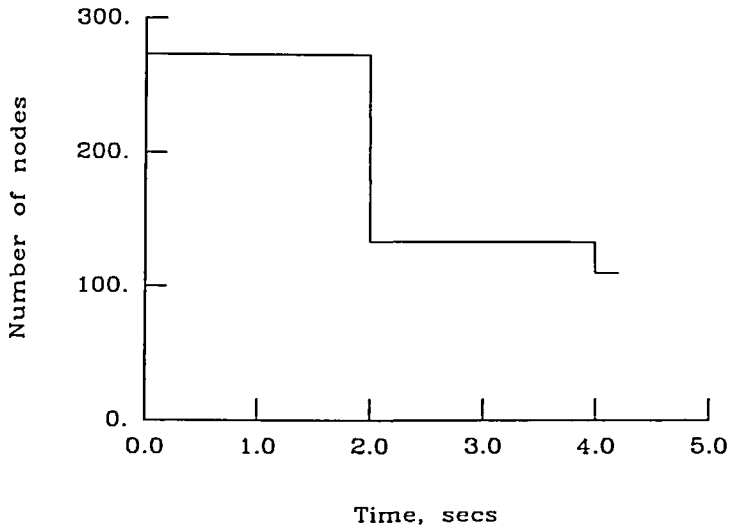

Figure 22 Nodes used for analysis as a function of time

Very steep gradients occur early in the transient and a fine mesh is needed to resolve the high temperature gradients. The initial mesh used for the analysis contains 273 uniformly spaced nodes. Adaptations are done every 2 sec and refinement and derefinement tolerances are set at 0.05 and 0.01 respectively. Refinement and derefinement tolerances are set lower for this problem to ensure adequate capture of high solution gradients at early time.

The finite element mesh and temperature contours at 2.2 sec and 4.2 sec are shown in *Figures 18* and *19*. Elements in the lower left corner of the domain that lie near the location of the heated section ($x = 0$, $y = 0.1$) are refined or held to their initial sizes. Elements at the top right corner where no appreciable gradients exist are coarsened continuously. The effectiveness of the refinement procedure is evaluated by the temperature distributions along the x and y axes at 4.2 sec in *Figures 20* and *21*. The symbols show the location of the nodes and indicate a clustering of elements where strong curvatures exist in the temperature profiles. The number of nodes used to model the leading edge during the transient response is plotted in *Figure 22* illustrating the rapid drop in the number of nodes used for description of the temperature profile.

CONCLUDING REMARKS

In this paper, an adaptive mesh refinement scheme is developed for modelling transient thermal problems. Nodeless variable finite elements with quadratic interpolation functions are used to obtain element temperature distributions. These distributions are essential for obtaining temperatures of new nodes when a mesh is refined. The finite element mesh is adapted at user-specified intervals during the transients, and nodeless variables in each element are used as refinement indicators at each adaptation level.

During transients, the finite element mesh is modified which results in an undesirable increase in the size of the global equations. Use of a nodal renumbering scheme reduces the bandwidth of these global equations which decreases both storage requirements and computation effort needed to solve the set of simultaneous equations. Typical reductions in bandwidth for the

examples presented range from factors of 10 to 20. Consequently, storage requirements for global arrays are also reduced by factors of up to 10.

The heat transfer examples in one and two dimensions illustrate the advantages of the adaptive scheme. The number of nodes used in the analysis is directly related to the severity of gradients as well as their locations. The overall accuracy of the analysis is maintained while the number of nodes usually decreases as the gradients in the solution decrease with time. The computational effort required to march out to a specified time in the analysis is reduced since elements are typically coarsened, causing the maximum allowable time step used in the analysis to be increased.

The examples presented in this paper illustrate the effectiveness of the adaptive unstructured finite element procedure for modelling transient heat transfer response accurately. Steep temperature gradients are handled efficiently with elements being enriched wherever needed. The number of elements needed to model the physical domain is minimized while spatial accuracy is maintained. The methodology used for transient thermal adaptation has good potential for extension into other disciplines, such as incompressible flow and viscoplasticity, where spatial resolution and temporal accuracy are of prime concern.

ACKNOWLEDGEMENT

The research of R. Ramakrishnan and E.A. Thornton was supported by research grant NSG-1321 through the Aerothermal Loads Branch at NASA Langley Research Center.

REFERENCES

1 Dechaumphai, P., Thornton, E. A. and Wieting, A. R. Fluid-thermal-structural study of aerodynamically heated leading edges, *J. Spacecraft Rockets*, **26**, 201–209 (1989)
2 Hogge, M. and Gerrekens, P. Steep gradient modeling in diffusion problems, *Numerical Methods in Heat Transfer*, (Ed. R. W. Lewis *et al.*), Vol. II, Wiley, Chichester (1982)
3 Adjerid, S. and Flaherty, J. E. A moving mesh finite element method with local refinement for parabolic partial differential equations, *Comp. Meth. Appl. Mech. Eng.* **55**, 3–26 (1986)
4 Thornton, E. A. and Vemaganti, G. An adaptive remeshing method for finite element thermal analysis, *AIAA J. Thermophys. Heat Transf.* **4**, 212–220 (1990)
5 Dechaumphai, P. and Morgan, K. Transient thermal-structural analysis using adaptive unstructured remeshing and mesh movement, *Thermal Structures and Materials for High-Speed Flight* (Ed. E. A. Thornton), Progress in Astronautics and Aeronautics 140, AIAA, Washington DC, pp. 205–227 (1992)
6 Demkowicz, L., Devloo, Ph. and Oden, J. T. On a *h*-type mesh refinement strategy based on minimization of interpolation errors, *Comp. Meth. Appl. Mech. Eng.* **53**, 67–89 (1985)
7 Ramakrishnan, R., Bey, K. S. and Thornton, E. A. Adaptive quadrilateral and triangular finite element scheme for compressible flows, *AIAA J.* **28**, 51–59 (1990)
8 Dechaumphai, P. and Thornton, E. A. Nodeless variable finite elements for improved thermal-structural analysis, *Proc. Int. Conf. Finite Element Methods, Shanghai*, Gordon and Breach, New York, pp. 139–144 (1982)
9 Huebner, K. H. and Thornton, E. A. *The Finite Element Method for Engineers*, Second Edition, John Wiley, Chichester (1982)
10 Zienkiewicz, O. C. *The Finite Element Method*, McGraw-Hill, New York, 3rd Edn (1977)
11 Collins, R. J. Bandwidth reduction by automatic renumbering, *Int. J. Num. Meth. Eng.* **6**, 345–356 (1973)
12 Lohner, R., Morgan, K. and Zienkiewicz, O. C. The solution of nonlinear hyperbolic equation systems by the finite element method, *Int. J. Num. Meth. Fluids*, **4** 1043–1063 (1984)
13 Carslaw, H. S. and Jaeger, J. C. *Conduction of Heat in Solids*, Oxford University Press, pp 112–113 (1980)
14 Churchill, R. V. and Brown, J. W. *Fourier Series and Boundary Value Problems*, Third Edition, McGraw-Hill, New York (1978)
15 Pandey, A. K., Dechaumphai, P. and Thornton, E. A. Finite element thermo-viscoplastic analysis of aerospace structures, *Thermal Structures and Materials for High-Speed Flight* (Ed. E. A. Thornton), Progress in Astronautics and Aeronautics 140, AIAA, Washington DC, pp. 229–253 (1992)